[6]A. A. Frost, M. Inokuti, and J. P. Lowe, J. Chem. Phys. 41, 482 (1964).

[7]A. K. Rajogopal, C. S. Shastry, and S. Radhakant, Nuovo Cimento Letters 4, 173 (1970); Phys. Rev. A 3, 234 (1971).

PHYSICAL REVIEW A VOLUME 4, NUMBER 3 SEPTEMBER 1971

Does the Coster-Kronig Transition Probability f_{23} Have a Radiative Component?*

Mau Hsiung Chen and Bernd Crasemann
Department of Physics, University of Oregon, Eugene, Oregon 97403

and

P. Venugopala Rao, J. M. Palms, and R. E. Wood
Department of Physics, Emory University, Atlanta, Georgia 30322

(Received 12 March 1971)

The radiative magnetic dipole transition rate between $2p_{3/2}$ and $2p_{1/2}$ single-particle electron states has been calculated with relativistic screened hydrogenic wave functions for seven elements with $70 \leq Z \leq 93$ and is found to contribute only $\sim 10^{-5}$ of the total L_2 level width. The result has been corroborated by an experimental study of the Pb M x-ray spectrum in coincidence with $K\alpha_1$ and $K\alpha_2$ x rays, establishing a limit $\omega_{23} \lesssim (1.4 \pm 3.0) \times 10^{-3}$ for the radiative part of the L_2-L_3X Coster-Kronig transition probability in Pb.

I. THEORY

Existing measurements[1–6] of the L_2-L_3X Coster-Kronig transition probability f_{23} for $Z \geq 70$ exceed theoretical results derived from screened hydrogenic wave functions[7] and from a self-consistent-field (SCF) approach[8] (Fig. 1). The question arises whether radiative spin-flip transitions could contribute measurably to f_{23}. The L_1-L_3 radiative Coster-Kronig transition has recently been observed,[9] as has the K-L_1 spin-flip transition.[10]

We calculate the radiative magnetic dipole transition rate between $2p_{3/2}$ and $2p_{1/2}$ single-particle electron states following the formalism of Scofield,[11] but with relativistic screened hydrogenic wave functions. The use of analytic wave functions is justified since only an order-of-magnitude result is desired. The initial and final states are characterized by the quantum numbers $\kappa_i = -2$, $\kappa_f = 1$ [$\kappa = \mp (j + \frac{1}{2})$ for $j = l \pm \frac{1}{2}$]. The transition rate is

$$\Gamma_{fi} = 2\alpha\omega^2 (2j_i + 1) f_1(m)$$
$$= 2\alpha\omega (2j_i + 1) B(-\kappa_i, \kappa_f, 1) R_1^2(m) , \tag{1}$$

where α is the fine-structure constant and ω is the transition energy, in units such that $\hbar = m = c = 1$. The quantity B, which vanishes unless $J = L + \bar{l}_i + l_f$ is even and L, j_i, and j_f form a triangle, is defined as

$$B(-\kappa_i, \kappa_f, L) = [(2\bar{l}_i + 1)(2l_f + 1)/L(L+1)]$$
$$\times C^2(\bar{l}_i, l_f, L; 0, 0) W^2(j_i \bar{l}_i j_f l_f; \tfrac{1}{2}L), \tag{2}$$

where $\bar{l} = -\kappa$ if $\kappa < 0$ and $\bar{l} = \kappa - 1$ if $\kappa > 0$. In the present case, $B(2, 1, 1) = \frac{1}{4}$, whence

$$\Gamma_{fi} = 2\alpha\omega R_1^2(m) . \tag{3}$$

The radial matrix element is

$$R_1(m) = (\kappa_i + \kappa_f) \int dr\, j_1(kr) (F_f G_i + G_f F_i)$$

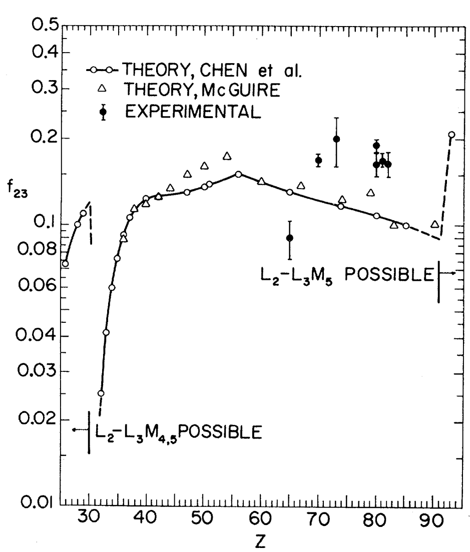

FIG. 1. Theoretical L_2-L_3X Coster-Kronig transition probability f_{23} calculated by Chen, Crasemann, and Kostroun (Ref. 7) from hydrogenic wave functions and by McGuire (Ref. 8) through an SCF approach, compared with experimental points (Refs. 1–6).

$$= -\int dr\, j_1(kr)\,(F_1 G_{-2} + G_1 F_{-2})\,. \quad (4)$$

With Slater-screened[12] hydrogenic bound-state wave functions,[13] we find

$$G_f F_i + F_f G_i = \alpha_1 r^\gamma e^{-\lambda r}(\beta_1 + \delta r) + \alpha_2 r^\gamma e^{-\lambda r}(\beta_2 + \delta r)\,, \quad (5)$$

where

$$\gamma = \gamma_{II} + \gamma_{III}, \qquad \gamma_i = (\kappa_i^2 - \xi_i^2)^{1/2}, \qquad \xi_i = \alpha Z_i^*$$

for the L_i state, and

$$\lambda = \lambda_{II} + \lambda_{III}, \qquad \lambda_i = (1 - W_i^2)^{1/2};$$

$$W_{II} = [\tfrac{1}{2}(1+\gamma_{II})]^{1/2}\,, \qquad W_{III} = \tfrac{1}{2}\gamma_{III}\,;$$

$$\alpha_1 = -N_{II} N_{III}(1+W_{II})^{1/2}(1-W_{III})^{1/2}\,,$$

$$\alpha_2 = -N_{II} N_{III}(1+W_{III})^{1/2}(1-W_{II})^{1/2}\,;$$

$$\beta_1 = 2(W_{II} - 1)\,, \quad \beta_2 = 2W_{II}\,; \quad (6)$$

$$\delta = 2(\lambda_{II} - \xi_{II})/(2\gamma_{II}+1)\,;$$

$$N_{II} = 2^{\gamma_{II}-1/2}\lambda_{II}^{\gamma_{II}+3/2}\{(2\gamma_{II}+1)/[\Gamma(2\gamma_{II}+1) \times \xi_{II}(\xi_{II} - \lambda_{II})]\}^{1/2}\,,$$

$$N_{III} = \xi_{III}^{\gamma_{III}+1/2}[2\Gamma(2\gamma_{III}+1)]^{-1/2}\,.$$

The matrix element $R_1(m)$ can then be expressed in simple closed form:

$$R_1(m) = -\frac{\alpha_1\beta_1 + \alpha_2\beta_2}{k^2}\,\frac{\Gamma(\gamma-1)\sin(\gamma-1)\theta}{(\lambda^2+k^2)^{(\gamma-1)/2}} - \frac{\alpha_1\delta + \alpha_2\delta}{k^2}\,\frac{\Gamma(\gamma)\sin(\gamma\theta)}{(\lambda^2+k^2)^{\gamma/2}} + \frac{\alpha_1\beta_1 + \alpha_2\beta_2}{k}\,\frac{\Gamma(\gamma)\cos\gamma\theta}{(\lambda^2+k^2)^{\gamma/2}} + \frac{\alpha_1\delta + \alpha_2\delta}{k}\,\frac{\Gamma(\gamma+1)\cos(\gamma+1)\theta}{(\lambda^2+k^2)^{(\gamma+1)/2}}\,, \quad (7)$$

where $\theta = \tan^{-1}(k/\lambda)$ and $k = \omega = E_f - E_i$, the energies E being the (absolute values of the) binding energies in the neutral atom[14] (in units of mc^2).

Numerical results for the $L_3 \to L_2$ $M1$ radiative transition probability are listed in Table I for selected atomic numbers.[15] For comparison, the total widths Γ^2 of atomic states characterized by an L_2 vacancy are also listed, based on an earlier computation.[7] It is seen that $L_3 \to L_2$ radiative transitions contribute only $\sim 10^{-5}$ of the total L_2 width.

II. EXPERIMENT

The result of the foregoing calculation was corroborated by an experimental search for 2.14-keV photons from the $L_3 \to L_2$ transition in the Pb x-ray spectrum that arises in the decay of Bi^{207}. The sought line falls into the M x-ray region. A sizable contribution from the radiative part ω_{23} of the Coster-Kronig probability $f_{23} = a_{23} + \omega_{23}$ would result in a difference in M-peak intensities in coincidence with $K\alpha_1$ and with $K\alpha_2$ x rays.

TABLE I. Calculated radiative L_2-L_3X Coster-Kronig widths Γ_R^{23} and total L_2 level widths Γ^2.

Element	Γ_R^{23} (eV)	Γ^2 (eV)[a]
$_{70}$Yb	6.40×10^{-6}	4.76[b]
$_{74}$W	1.48×10^{-5}	5.151
$_{78}$Pt	2.97×10^{-5}	5.64[b]
$_{80}$Hg	4.23×10^{-5}	5.942
$_{82}$Pb	5.89×10^{-5}	6.25[b]
$_{85}$At	9.81×10^{-5}	6.779
$_{93}$Np	3.58×10^{-4}	9.842

[a]From Ref. 7. [b]Interpolated.

To derive the necessary equations for the interpretation of the experiment, the following definitions are introduced:

$C_{MK\alpha_1}$ = counting rate of M x rays in coincidence with $K\alpha_1$ x rays;

$C_{MK\alpha_2}$ = counting rate of M x rays in coincidence with $K\alpha_2$ x rays;

$C_{K\alpha_1}$ = counting rate of $K\alpha_1$ x rays in the $K\alpha_1$ gate;

$C_{K\alpha_2}$ = counting rate of $K\alpha_2$ x rays in the $K\alpha_2$ gate[16];

n_{L_2M} = number of M vacancies produced in filling an L_2 vacancy;

n_{L_3M} = number of M vacancies produced in filling an L_3 vacancy;

ω_{L_2M} = average M-shell fluorescence yield for the M-vacancy distribution created when an L_2 vacancy is filled;

ω_{L_3M} = average M-shell fluorescence yield for the M-vacancy distribution created when an L_3 vacancy is filled.

The measured coincidence counting rates are given by

$$C_{MK\alpha_1} = C_{K\alpha_1} n_{L_3M}\,\omega_{L_3M}\,(\epsilon\Omega f)_M\,, \quad (8)$$

$$C_{MK\alpha_2} = C_{K\alpha_2}[n_{L_2M}\,\omega_{L_2M} + f_{23} n_{L_3M}\,\omega_{L_3M} + \omega_{23}](\epsilon\Omega f)_M\,, \quad (9)$$

where $(\epsilon\Omega f)_M$ refers to efficiency, solid angle, and attenuation correction. Equations (8) and (9) do not contain terms that account for nuclear cascading. In the case of Bi^{207}, such nuclear cascading is very small, because of the long lifetime of the 1633-keV state involved in the major decay mode.

We now take $\omega_{L_2M} \cong \omega_{L_3M} = \bar{\omega}_M$. This assumption is based on a detailed estimate of the vacancy distributions, and on the observation[17] that most M vacancies tend to be shifted to the M_4 and M_5 subshells by Coster-Kronig transitions, and that the

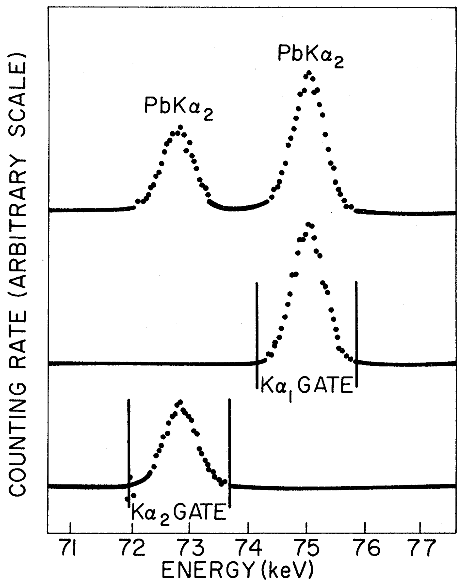

FIG. 2. Lead $K\alpha$ x-ray spectrum from Bi^{207} decay. Positions of gates employed in coincidence experiments are indicated.

fluorescence yields of these two subshells appear to be nearly the same. Dividing Eq. (9) by Eq. (8), we then find

$$\left[\frac{C_{MK\alpha_2}}{C_{MK\alpha_1}}\;\frac{C_{K\alpha_1}}{C_{K\alpha_2}}\right]-\left[\frac{n_{L_2M}}{n_{L_3M}}+f_{23}\right]=\frac{\omega_{23}}{n_{L_3M}\bar{\omega}_M}\;. \quad (10)$$

The vacancy numbers n_{L_2M} and n_{L_3M} can be estimated from L_2 and L_3 x-ray emission rates,[11] Auger-electron line intensities,[18] and measured Coster-Kronig transition probabilities,[4,19] with the result $n_{L_2M}\cong 0.95$ and $n_{L_3M}\cong 1.13$.[20] For the pertinent average M-shell fluorescence yield, we adopt $\bar{\omega}_M = 0.030 \pm 0.007$ from the work of Jopson *et al.*[21] and of Konstantinov and Sazonova,[22] and we use[4,19] $f_{23} = 0.164 \pm 0.016$.

Lead M and L x-ray spectra from a thin Bi^{207} source were measured with a Kevex Si(Li) detector [dead layer < 0.3 μ, 0.05-mm Be window, resolution 260 eV full width at half-maximum (FWHM) at 6.4 keV] in coincidence ($2\tau = 800$ nsec) with $K\alpha_1$ or $K\alpha_2$ x rays measured with a Ge(Li) detector (resolution 480 eV FWHM at 14.4 keV). The $K\alpha$ x-ray spectrum is shown in Fig. 2. Typical M and L x-ray spectra in coincidence with $K\alpha_1$ and $K\alpha_2$ x rays are reproduced in Fig. 3. Also shown in Fig. 3 is the spectrum of M and L x rays in coincidence with $K\beta_{1,3}$ x rays, which arise from $M_{2,3}\to K$ transitions. The smallness of the peak at 3.1 keV shows that $M_{2,3}$ vacancies are not often filled radiatively, but most frequently are transferred to the $M_{4,5}$ subshells by Coster-Kronig transitions. Radiative filling of the $M_{4,5}$ vacancies results in the prominent peak at ~ 2.5 keV. This observation supports our assumption underlying the formulation of Eq. (10) that $\omega_{L_2M}\cong\omega_{L_3M}$.

The result of the coincidence measurements is

$$C_{MK\alpha_2}C_{K\alpha_1}/C_{MK\alpha_1}C_{K\alpha_2}=1.044\pm 0.075\,,$$

whence, by Eq. (10), the radiative L_2-L_3X Coster-Kronig transition probability in Pb is

$$\omega_{23} \lesssim (1.4 \pm 3.0)\times 10^{-3}\,.$$

This limit on ω_{23} corresponds to a limit

$$\Gamma_R^{23} \lesssim (0.9 \pm 1.9)\times 10^{-2}\ \mathrm{eV}$$

on the radiative L_2-L_3X partial width, which is compatible with the result of the calculation in Sec. I: The theoretical partial width is approximately 200 times smaller than the experimentally established upper limit. Clearly, radiative transitions do not account for an appreciable part of f_{23}.

A part of the discrepancy between theoretical and experimental f_{23} values that prompted this investigation has very recently been traced to a systematic experimental error due to the presence of the unresolved $L\eta$ line in the $L\alpha$ x-ray group.[23] The remaining difference may well arise from the approximate nature of the wave functions used by Chen *et al.*[7] and of McGuire's approach,[8] and may disappear when calculations with more realistic numerical wave functions are performed.

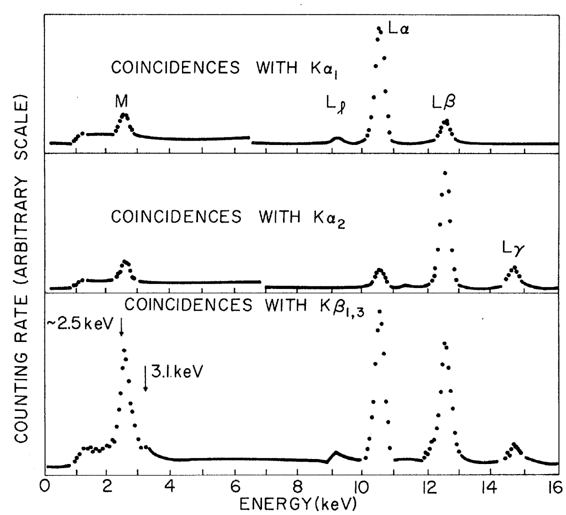

FIG. 3. Lead M and L x rays from Bi^{207} decay.

*Work supported in part by the U.S. Atomic Energy Commission and by USAROD Basic Research Grant No. DA-ARO-D31-124-70-G78.

[1]S. Mohan, H. U. Freund, R. W. Fink, and P. Venugopala Rao, Phys. Rev. C 1, 254 (1970).

[2]P. Venugopala Rao and B. Crasemann, Phys. Rev. 139, A1926 (1965).

[3]S. Mohan, R. W. Fink, R. E. Wood, J. M. Palms, and P. Venugopala Rao, Z. Physik 239, 423 (1970).

[4]P. Venugopala Rao, R. E. Wood, J. M. Palms, and R. W. Fink, Phys. Rev. 178, 1997 (1969).

[5]J. M. Palms, R. R. Wood, P. Venugopala Rao, and V. O. Kostroun, Phys. Rev. C 2, 592 (1970).

[6]R. E. Wood, J. M. Palms, and P. Venugopala Rao, Phys. Rev. 187, 1497 (1969).

[7]M. H. Chen, B. Crasemann, and V. O. Kostroun, University of Oregon Nuclear Physics Report No. RLO-1925-50, 1971 (unpublished).

[8]E. J. McGuire, Phys. Rev. A 3, 587 (1971).

[9]H. U. Freund, E. Karttunen, and R. W. Fink, Bull. Am. Phys. Soc. 15, 1305 (1970).

[10]R. K. Smither, M. S. Freedman, and F. T. Porter, Phys. Letters 32A, 405 (1970); F. Boehm, *ibid.* 33A, 417 (1970).

[11]J. H. Scofield, Phys. Rev. 179, 9 (1969).

[12]V. O. Kostroun, M. H. Chen, and B. Crasemann, Phys. Rev. A 3, 533 (1971).

[13]M. E. Rose, *Relativistic Electron Theory* (Wiley, New York, 1961), Sec. 29.

[14]J. A. Bearden and A. F. Burr, Rev. Mod. Phys. 39, 125 (1967).

[15]After completing these calculations, we found that unpublished results by H. R. Rosner and C. P. Bhalla, based on relativistic Hartree-Fock-Slater wave functions, agree closely with some of the transition probabilities obtained in the present work.

[16]The counting rate in the $K\alpha_2$ gate is corrected for counts due to the tail of the $K\alpha_1$ x-ray photopeak; see Ref. 4.

[17]E. Karttunen, Ph.D. thesis (Georgia Institute of Technology, 1971) (unpublished).

[18]S. K. Haynes, M. Velinsky, and L. J. Velinsky, Nucl. Phys. A90, 573 (1967).

[19]The value of f_{23} for Pb was remeasured in the course of the present experiment, with exactly the same result obtained previously (Ref. 4), viz., $f_{23} = 0.164 \pm 0.016$.

[20]Our value of n_{L_2M} includes the effect of L_2-M radiative and L_2-MM, L_2MX, and L_2-L_3M radiationless transitions, but does not include the effect of subsequent transitions to the L_3 vacancy created by the L_2-L_3M Coster-Kronig transitions.

[21]R. C. Jopson, Hans Mark, C. D. Swift, and M. A. Williamson, Phys. Rev. 137, A1353 (1965).

[22]A. A. Konstantinov and T. E. Sazonova, Bull. Acad. Sci. USSR Phys. Ser. 32, 581 (1968).

[23]J. C. McGeorge, S. Mohan, and R. W. Fink (unpublished).

PHYSICAL REVIEW A VOLUME 4, NUMBER 3 SEPTEMBER 1971

Nuclear-Spin Inertia and Pressure Broadening of $^2P_{1/2}$ Hanle-Effect Signals*

B. R. Bulos and W. Happer

Columbia Radiation Laboratory, Department of Physics, Columbia University, New York, New York 10027

(Received 14 April 1971)

Hanle-effect measurements yield values for the collisional depolarization rates of $^2P_{1/2}$ excited atomic states that are about three times too small unless one explicitly includes the effects of nuclear spin. The broadening also becomes a nonlinear function of foreign-gas pressure. We present experimental evidence for nuclear-spin effects on pressure-broadened Hanle-effect signals of Rb^{85} and Rb^{87} in helium.

Well-isolated $^2P_{1/2}$ atomic states, such as the $5\,^2P_{1/2}$ state of rubidium, the $6\,^2P_{1/2}$ state of cesium, or the $6\,^2P_{1/2}$ state of thallium are known to have anomalously small collisional depolarization rates in inert gases. Franz[1] and Gallagher[2] have pointed out that this is because the dominant forces during an interatomic collision are of an electrostatic nature and cannot exert torques on a $^2P_{1/2}$ state. However, a $^2P_{1/2}$ state can be depolarized by virtual transitions to the neighboring $^2P_{3/2}$ state; and, consequently, when the fine-structure splitting of the P doublet is small, as is the case in potassium and sodium, the depolarization rates are large. The most detailed experimental studies of collisional depolarization of $^2P_{1/2}$ states are those of Gallagher,[3] whose results are summarized in Table I. Gallagher's quoted depolarization cross sections are indeed quite small compared to the corresponding $^2P_{3/2}$ depolarization cross sections, which are typically on the order of 10^{-14} cm^2. In this paper we would like to point out that Gallagher's quoted cross sections actually exaggerate the smallness of the depolarization cross sections by a factor of about 3. This is because the width of Hanle-effect signals is narrowed by certain nuclear-spin effects that have nothing to do with the true electronic depolarization process.

It is well known that the nucleus is essentially